Protein hydrogen exchange: Testing current models

John J. Skinner,[1]*† Woon K. Lim,[2] Sabrina Bédard,[1] Ben E. Black,[1] and S. Walter Englander[1]

[1]Johnson Research Foundation, Department of Biochemistry and Biophysics, Perelman School of Medicine, University of Pennsylvania, Philadelphia, Pennsylvania 19104-6059

[2]Department of Molecular Biology, College of Natural Sciences, Pusan National University, 30 Jangjeon-dong, Keumjeong-gu Busan 609-735, South Korea

Received 13 February 2012; Accepted 9 April 2012
DOI: 10.1002/pro.2082
Published online 27 April 2012 proteinscience.org

Abstract: To investigate the determinants of protein hydrogen exchange (HX), HX rates of most of the backbone amide hydrogens of Staphylococcal nuclease were measured by NMR methods. A modified analysis was used to improve accuracy for the faster hydrogens. HX rates of both near surface and well buried hydrogens are spread over more than 7 orders of magnitude. These results were compared with previous hypotheses for HX rate determination. Contrary to a common assumption, proximity to the surface of the native protein does not usually produce fast exchange. The slow HX rates for unprotected surface hydrogens are not well explained by local electrostatic field. The ability of buried hydrogens to exchange is not explained by a solvent penetration mechanism. The exchange rates of structurally protected hydrogens are not well predicted by algorithms that depend only on local interactions or only on transient unfolding reactions. These observations identify some of the present difficulties of HX rate prediction and suggest the need for returning to a detailed hydrogen by hydrogen analysis to examine the bases of structure-rate relationships, as described in the companion paper (Skinner et al., Protein Sci 2012;21:996–1005).

Keywords: hydrogen exchange; HX; electrostatics; static and dynamic; protein folding; cleanex-PM; Staphylococcal nuclease; EX1

Introduction

The main chain amide hydrogens of proteins engage in continual exchange with the hydrogens of solvent water. Proton transfer chemistry is well understood,[1] and the hydrogen exchange (HX) rates of exposed amides in structureless polypeptides—in any sequence, ambient condition, and isotope combination—can be accurately predicted.[2,3] Amide hydrogens in structured proteins exchange more slowly, over a great range of rates that depend on and therefore can provide information about biophysical properties (structure, stability, dynamics, energetics) and functional properties (interaction, structure change, folding) resolved to the individual amino acid level. To most effectively exploit this rich source of information, it will be necessary to understand the static and dynamic determinants of HX behavior. The common presumption that the determinants are well understood is far from true. These uncertainties limit the interpretive power of the many structural and functional HX studies that are now being reported.

In formative work before the first protein structure had been solved, Linderstrøm-Lang explored

Additional Supporting Information may be found in the online version of this article.

†Current address: Department of Biochemistry and Molecular Biology, University of Chicago, Chicago, Illinois 60637.

Grant sponsor: NIH; Grant numbers: GM031847, GM082989; Grant sponsor: NSF; Grant numbers: MCB1020649; Grant sponsor: Mathers Foundation; Burroughs Welcome Fund (Career Award in the Biomedical Science); Rita Allen Foundation Scholars Award; 2-year research grant from Pusan National University.

*Correspondence to: John J. Skinner, GCIS Room W107E, 929 E. 57th St., Chicago, IL 60637. skinnerj@uchicago.edu

$$\text{Closed} \underset{k_{cl}}{\overset{k_{op}}{\rightleftarrows}} \text{open} \xrightarrow{k_{ch}} \text{exchange}$$

Scheme 1. Linderstrøm–Lang kinetic model for exchange of protected hydrogens.

protein HX with the intention of looking for Pauling's H-bonded helices and sheets. Lang took the view that the slowly exchanging hydrogens found by his group did indeed represent Pauling's H-bonded structures. He proposed a straightforward phenomenological model, namely that the exchange process requires structural protection to be relieved by some dynamic structural event.[4–6] The picture is commonly represented as in Scheme 1 where k_{op} and k_{cl} are structural opening and reclosing rates, and k_{ch} is the chemical rate expected for exposed hydrogens.[2]

Scheme 1 is wholly kinetic in nature and has no structural content. Over the years, the search for the physical determinants has elicited a number of proposals. In general, prior workers have attempted top down strategies. Some structure-based determinant of HX rate is proposed and then an HX database is tested for correlation with that factor. To examine these uncertainties, we obtained a large HX dataset for most of the amide hydrogens of the Staphylococcal nuclease (SN) protein. We used a double mutant (P117G/H124L) with increased stability so that most HX is not controlled by the global unfolding reaction. SN has extensive alpha and beta structural content, its detailed atomic level structure and biophysical properties are well known, and previous experiments specify the relative size of structural excursions that allow the exchange of many individual SN hydrogens.[7,8] These comprehensive data provide a resource for examining the static and dynamic structural factors that determine protein HX rates.

We used these data to test models previously proposed in attempts to understand protein HX in terms of known structure and calculated properties. Accessibility-penetration models suppose that solvent accessible hydrogens placed at the protein surface will exchange rapidly and that the slower exchange of more buried hydrogens depends on the entry of water or the HX catalysts, hydroxide and hydronium ion, into the protein matrix.[9–11] Electrostatic field has been suggested to play a major role in modulating the HX rate of amides exposed to solvent at the protein surface.[12–15] For more buried hydrogens, predictions of HX rates based on local interaction density and the calculation of structural dynamics have been attempted.[16–29,30–34] We compare these models to SN HX data and discuss the problematic issues.

Results

We assigned the NMR spectrum of SN[8] and used this information to measure HX rates for 109 out of 143 nonproline backbone amide hydrogens and a tryptophan indole ring NH using the Cleanex-PM NMR method[35] for fast exchanging amides (1–100 s^{-1}) and 2D HSQC NMR for slower ones (10^{-3} to 10^{-7} s^{-1}).[8] HX was measured at closely spaced intervals from pH 4.9 to 11.3 to bring faster and slower rates into the laboratory time window. SN stability remains constant below pH 10 (Ref. 8), which allows measured HX rates over a very wide pH range to be directly compared, as in Figure 1.

Data validation

HX rates for P117G/H124L SN are listed in Supporting Information Table S1 in terms of their structural protection factors (P_f) under EX2 conditions. The accuracy of the measured rates was checked in several ways.

Previous calibrations make it possible to predict HX rates for main chain amides in unstructured polypeptides based on primary amino acid sequence and ambient conditions.[2,3] For seven of the eight amides measured on unstructured SN segments (residues 2 and 5 at the N-terminus and 144–149 at the C-terminus), rates agree with predicted values to better than twofold. The one exception, Thr2, exchanges rapidly, 10-fold faster than predicted in Ref. 2, apparently due to the positive N-terminal charge, as might have been expected (see Table 1 in Ref. 36). This is especially important for the back exchange problem in HX mass spectrometry analysis, which deals with many peptide fragments, all having an N-terminal charge.

Under our conditions amide HX is catalyzed only by hydroxide, therefore HX rates are ideally expected to increase by a factor of 10 per pH unit. Figure 1 shows that multiple independently

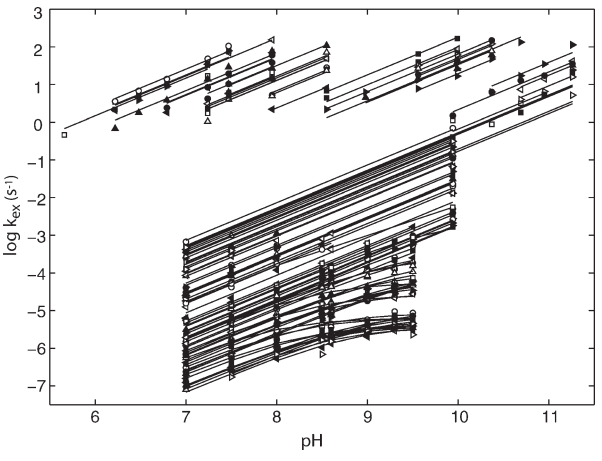

Figure 1. ^{1}H-^{1}H (Cleanex-PM) and ^{1}H-^{2}H (HSQC) exchange rates as a function of pH. Lines through the data for each hydrogen measured with EX2 behavior are drawn with unit slope. Residues with an EX2 to EX1 transition are fit to the standard equation that describes that behavior.[5] The various symbols are used simply for clarity.

measured data points for any given amide hydrogen fall accurately on a line with unit slope (average deviation 14%). In addition, the fast hydrogens measured by CLEANEX-PM and analyzed by the improved method, described in Materials and Methods, match this expected EX2 behavior. Some of the very slowest amides are exceptional. They transition at high pH toward a pH-independent EX1 mechanism,[8] and so provide important additional information about structural dynamics as described below.

Six residues could be measured by both the Cleanex-PM and HSQC methods, although at different conditions. These rates can be compared by applying the expected pH dependence[2] and isotope effects.[3] Rates for five of the six sites agree within an average deviation of 30%. The one outlier, Phe61, could only be measured by Cleanex-PM at pH 11.26 where rates are questionable due to protein destabilization.

In summary, measured HX rates were checked by comparing them with predicted rates for unstructured residues, with their expected dependence on pH over a wide pH range, and with rates measured by different methods. These tests confirm the accuracy of the results.

HX mechanism: Solvent accessibility

It is often stated that HX rate measures solvent accessibility, which leads to the expectation that protein surface hydrogens will exchange at rates close to those calibrated for amides in unstructured polypeptides.[11,37] The results in Figure 2 are not consistent with this view. Figure 2 replots the data in Figure 1 in terms of measured HX protection factor (P_f) versus distance to the protein surface. Unprotected surface hydrogens on unstructured SN segments at the N- and C-termini (plotted at 0.7 Å) do exchange rapidly, at their expected unprotected rates with protection factor ~1 (log $P_f \sim 0$). Unprotected surface hydrogens on structured segments (plotted at ~2 Å) exchange more slowly, by up to 40-fold. Other near-surface but H-bonded hydrogens on the solvent-exposed surfaces of regular secondary structures or loops can exchange as slowly as deeply buried ones.

In summary, fast exchanging hydrogens that approximate the expected free peptide rate are placed only at the protein surface, but many others at the protein surface exchange far more slowly. The discriminating factor is protection by H-bonding.

HX mechanism: Solvent penetration

A hypothesis related to the solvent accessibility view is that slow exchange represents buried hydrogens and the HX process requires the penetration of HX catalyst into the protein matrix. This view has been

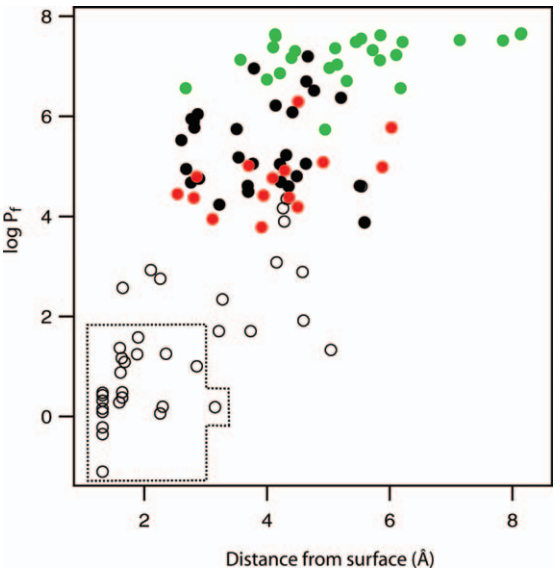

Figure 2. Log of HX protection factor as a function of distance to the SN surface. Distance was measured from the hydrogen center of mass (1.3 Å radius) to the aqueous surface generated by a rolling ball analysis (1.4 Å radius). Symbols indicate: HX measured by the Cleanex-PM method (open circles); amides known to exchange by way of a cooperative unfolding reaction (green); amides known to exchange by a local fluctuation pathway (red); HX pathway unknown (black). Unprotected hydrogens on unstructured and structured SN segments (boxed) are plotted at 0.7 and ~2 Å, respectively.

taken over the years by many authors. Figure 2 shows that this view is incorrect. Many near-surface hydrogens, where the concept of penetration has little meaning, can exchange as slowly as well buried ones. For internal hydrogens, the degree of HX protection has no significant dependence on depth of burial.

Further, many of the slowest hydrogens are known to exchange by way of sizeable unfolding reactions rather than being reached *in situ* by incoming solvent species. Their exchange is sharply accelerated by low concentrations of added denaturant,[7,38] which promotes unfolding reactions, even under fully native conditions far below the melting concentration.[39] In agreement, the unfolding reaction that modulates HX of the slowest SN hydrogens (EX2 region) has a computed free energy equal to global unfolding ($\Delta G_{op} = -RT \ln k_{op} = -RT \ln k_{ex}/k_{ch} = 10$ kcal mol^{-1}).[8] In addition, the HX rate for many very slow hydrogens is seen (Fig. 1) to roll over at high pH and approach pH-independent EX1 behavior. This indicates exchange by way of dynamic unfolding/refolding reactions that reclose relatively slowly (>1 ms) and therefore represent sizeable unfoldings. Thus many slow SN hydrogens, which should be prime candidates for exchange by way of a penetration mechanism, instead exchange by way of sizeable unfolding reactions.

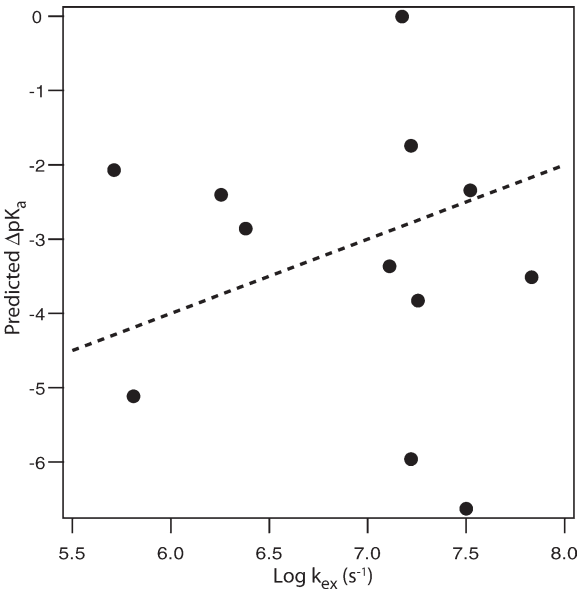

Figure 3. Comparison of the slowed exchange of exposed amides on structured segments (>0.5 Å^2 SASA) with predicted ΔpK_a values from electrostatic deprotonation calculations.

These results limit the HX rate that any penetration mechanism could mediate. It must be slower than the slowest hydrogens measured here, namely more than eight orders of magnitude slower than the structurally unhindered rate of fully exposed amides. A similar conclusion holds for the possibility of any direct amide to solvent exchange mechanism.

HX mechanism: Electrostatic field

Some unprotected amide hydrogens at the protein surface exchange more slowly than expected for freely solvent exposed amides[2] by up to 40-fold. A more extreme result has been described by the LeMaster group who reported the retardation of exchange rates for apparently solvent accessible amides[40] by up to a billion-fold in one case.[41] They attributed this behavior to electrostatic effects on the relative acidity of amides (pK_a); that is, on the intrinsic exchange rate, k_{ch}, of unprotected amides. It was assumed that amides with a solvent accessible surface area (SASA) $\geq$ 0.5 Å^2 are unprotected and have an unhindered rate of encounter with hydroxide catalyst. In this case, the excess slowing will depend only on the unfavorable proton transfer equilibrium within the encounter complex, dependent on pK_a.[1] To test this possibility, they used Poisson–Boltzmann continuum dielectric calculations to evaluate the change in amide pK_a values due to local formal and partial charges. They plotted the calculated ΔpK_a against measured HX rates, and fit several factors to improve the correlation.

We repeated electrostatic calculations for the proteins studied by the LeMaster group using their parameters.[40,41] Our calculations for CI2, FKBP12, and rubredoxin essentially duplicate their results. Results for the same calculations applied to the slow amide protons of SN with computed SASA > 0.5 Å^2 are in Figure 3. The measured HX rates show no correlation with calculated electrostatic field. It is notable that the computed ΔpK_a range is about as large as was computed for other proteins, but the range of measured rates is far smaller. We have not attempted to correlate this narrow range of rates with detailed determinants. The much slower rates reported by LeMaster *et al*. are due to a small number of outliers, as described in Discussion.

HX mechanism: Predictions from packing density and dynamics

Many workers have attempted predictive calculations that might correlate HX rates with static and dynamic structural determinants.[16–34,42] Difficulties arise because, unlike the rapid dynamic fluctuations that have received much attention in recent years, the fluctuations that determine HX behavior are rare, with populations from 10^{-1} to 10^{-10} relative to the native state and with time scales from ms to months. Various calculational approaches have been explored. The determinants considered range from immediately local residue–residue interactions to the ensemble of large segmental unfolding reactions. In spite of the very different factors that determine the different calculations and the varied criteria used for translating calculated results into HX rates, these efforts generally report good predictive results.

Illustrative examples in Figure 4 are taken from calculations that focus either on immediately local interaction density or on distributed segmental unfolding reactions. The presentation of results has usually used the format in Figure 4(a), which plots measured and predicted HX rates against amino acid sequence. This presentation tends to exaggerate the quality of the prediction. For example Figure 4(b,c) shows the same results in the format of a correlation scatter plot. In the horizontal dimension, the type of presentation in Figure 4(a) simply shows that the predictive algorithm being tested is generally able to distinguish residues in secondary structural elements where HX tends to be slow from those in intervening loop regions. The vertical dimension of the plot is often scaled to the stability of the protein so that the maximum protection factor enters as an adjustable parameter [although this is not true for the red curve in Fig. 4(a)].

Discussion

To appraise the continuing effort to understand protein HX behavior, we compared expectations of major current hypotheses with an extensive SN HX dataset.

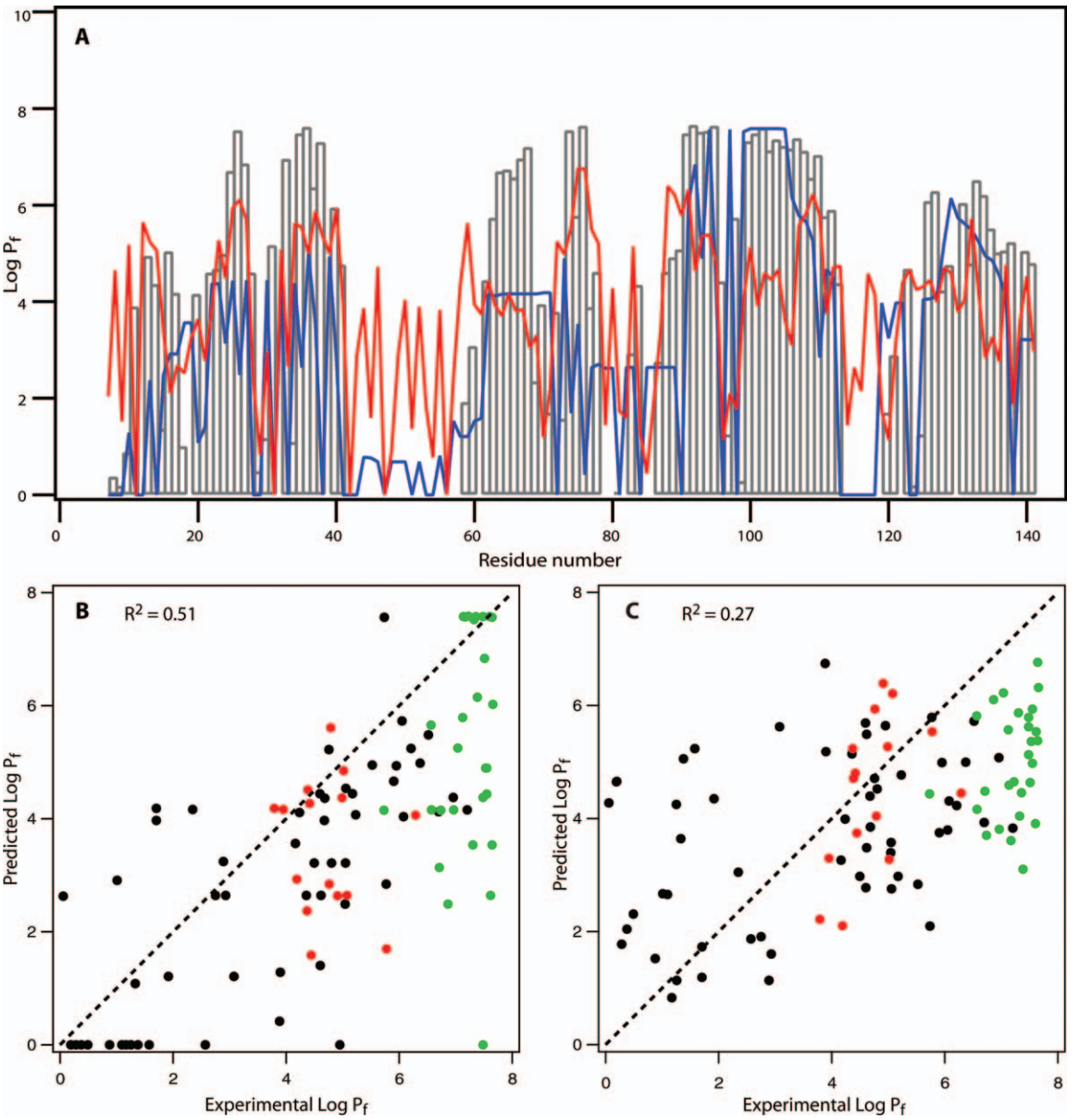

Figure 4. Comparisons of measured and predicted SN HX. A. Open bars represent measured P_f values. Predicted P_f values based on the density of local contacts in the static SN structure and more distributed segmental unfolding are displayed, respectively, by red lines (provided by M. Vendruscolo), and by blue lines (from the COREX program, provided by L. Tong and V. Hilser). The same data are also shown as correlation plots in panels B and C, respectively. R^2 values are calculated relative to the best fit lines (not shown) rather than to the identity line (dashed). Symbols in B and C indicate hydrogens known to exchange by local fluctuations (red), by larger unfolding (green), and those that are unknown (black). The local interaction model[26–29] was originally intended to translate HX data into constraints to help compute ensembles that produce the observed HX, and might not work when applied to structures of folded proteins. A previous COREX comparison[42] used an HX dataset for a less stable version of SN (WT) where the exchange of many of the measured hydrogens is dominated by global unfolding. The more stable SN variant used here provides increased dynamic range and more examples of exchange that depends on local fluctuations.

Static accessibility and burial

Over the years, many workers have taken the intuitive view that HX slowing depends on relative accessibility to solvent in the static protein structure. We find that hydrogens on dynamically unstructured protein segments in contact with solvent do exchange at their expected free peptide rate. Other unprotected hydrogens placed on structured segments exchange more slowly than expected by up to 40-fold. Hydrogens at the solvent interface that are sterically protected by H-bonding can exchange more slowly by many orders of magnitude. They require dynamic perturbations that separate the protecting H-bond and expose the hydrogen to attack by HX catalyst.

The same is undoubtedly true for H-bonded hydrogens that are buried, even if they could be

reached by incoming solvent species. For buried hydrogens, any solvent penetration model would predict a correlation between HX protection and distance to the aqueous surface. In fact, the results in Figure 2 show that when unprotected hydrogens are excluded, the correlation with depth of burial is close to zero. The most buried amides that are the prime candidates for a penetration mechanism instead tend to exchange by way of unfolding reactions. These results place an upper limit on the rate for any possible penetration mechanism that is, for practical purposes, negligible.

Slow surface HX and electrostatic field

Figure 3 tests the proposal that the slow exchange of supposedly unprotected surface hydrogens, defined by SASA > 0.5 Å^2, might be explained by local electrostatic field.[40,41] The unprotected solvent exposed hydrogens on structured segments of SN can exchange moderately slowly but they show no significant correlation with computed electrostatic field (Fig. 3).

It is noteworthy that the rate versus field correlations found in previous studies with other proteins[40,41] depend heavily on a few very slow hydrogens that anchor the correlation curves. Is it possible that these hydrogens are structurally protected in some nonobvious way? A companion study[43] reveals that structurally bound water molecules protect a number of SN amides from HX. When solvent is treated as a continuum as in previous studies, the usual rolling ball SASA analysis will fail to distinguish near-surface structurally bound waters from free solvent. We considered prior work from this point of view. Analysis shows that some slowly exchanging hydrogens considered to be solvent exposed in the previous studies[40,41] are H-bonded to crystallographically defined water molecules held in place by specific protein interactions.

In CI2,[40] the slowest supposedly unprotected hydrogen (Arg62) is H-bonded to a crystallographically defined water molecule that also H-bonds to a main chain carbonyl between two beta strands. Other slow amides (Val31, Ile44, and Asp45) are H-bonded to defined waters that also donate H-bonds to main chain and side chain carbonyls. These waters could not be simply replaced with hydroxide catalyst[44] without some structural adaptation, and therefore must offer protection against HX. Five of the remaining 10 amides in CI2 that contribute to the rate versus field correlation are in a loop that interacts with a neighboring protein in the crystal. This makes uncertain their local environment and therefore the calculated field in the monomeric solution condition of the HX experiments.

In rubredoxin,[41] the very slowly exchanging Lys46 amide hydrogen is H-bonded to a defined water molecule that is held also by H-bonding to main chain carbonyls. The Asp14 amide is H-bonded to a protecting water that is also H-bonded to a main chain carbonyl and to a tyrosine side chain OH. The slowest hydrogen, on Val38, is H-bonded to a defined water molecule that is involved in a network of water molecules held in a cleft between Val38 and an external loop. In other cases where apparently exposed but slowly exchanging hydrogens help to anchor the rate-field correlation curve, the slow amides are also H-bonded to defined water molecules held in place by H-bonding to protein groups.

These interactions make exchange slow by blocking encounter with hydroxide HX catalyst, and they ensure that the Poisson–Boltzmann calculation will compute a strongly unfavorable deprotonation environment. When the slowly exchanging hydrogens identified as structurally protected in this way are removed from the correlation curves, one finds a situation like that seen for SN (Fig. 3). Only a much smaller range of HX rates due to clearly unprotected solvent exposed hydrogens remains, and a lack of correlation between HX rate and electrostatic field is apparent.

Previous workers have found that exchange rates of freely exposed amides can be affected by and in some cases explained by local electrostatic effects.[13,45,46] The question considered here is whether such effects account for the surprisingly large HX retardation seen for some exposed protein surface amides. Considerations just described question the reality of the correlation inferred before. Some re-examination of factors in the analysis may be useful. This especially includes not only explicitly bound water molecules but also the use of a 0.5 Å^2 filter in a continuum water calculation to identify freely accessible hydrogens, and the use of an internal dielectric model for the protein with $\varepsilon = 3$ since the large dynamic range calculated for pK_a varies linearly with $1/\varepsilon$.

Structural dynamics

The evidence against exchange *in situ* for both surface and buried hydrogens, presented above, favors a dominant role for dynamic structural perturbations, as in the general Linderstrøm-Lang model (Scheme 1). In recent years, much effort has been devoted to the computation of the protein dynamic ensemble, especially to examine the implications for protein biophysics, folding, and function. An excellent test for these methodologies is their ability to predict amino acid resolved HX behavior.

The present results illustrate some continuing problems. Any given hydrogen may exchange by way of different kinds of dynamic exposure reactions ranging from small local fluctuations to whole molecule unfolding. Local fluctuations depend mainly on local interactions between immediate neighbors. Unfolding reactions depend on the network of interactions that stabilize a larger region of the protein. Predictive algorithms focused on local interactions seem unlikely

to predict exchange by way of segmental unfolding reactions that depend on more distributed interactions, or by the displacement of the H-bond acceptor rather than the exchanging residue itself. Similarly, exposure by small local fluctuations seems unlikely to be captured by the thermodynamic solvent exposure parameters used to calculate the probability of sizeable unfolding reactions. The difficulty of the problem is compounded by the fact that subtle effects, and even distant effects, may determine the pathway that dominates. For example, the mutation of a cis-proline residue in our mutant SN variant greatly increases protein stability and causes many distant residues to switch from a dependence on global unfolding to more local perturbations.

A successful HX prediction algorithm will have to take into account the different HX pathways for reaching the exchange competent state. It will be necessary to parameterize such an algorithm against data that distinguish HX due to local fluctuations and unfolding reactions. It will also be necessary to implement correct criteria for distinguishing exchange competent and exchange incompetent states. Some groups have defined exchange competence by H-bonding geometry.[17,20,22] Others have used solvent accessibility.[18,21,47] We find that even H-bonding to a water molecule does not always correspond to HX competence,[43] which ultimately depends on the ability to form an H-bond to HX catalyst, typically the solvent hydroxide ion.

Conclusions

Current models for protein HX behavior derive from a top down approach in which some static determinant or dynamic mechanism or calculational approach is proposed and then an HX database is tested for correlation with that factor. This article compares detailed HX results with major current models. The results suggest the value of returning to primary residue-resolved HX data, in a bottom up analysis, in order to compare HX behavior on a hydrogen by hydrogen basis with detailed structure and the HX behavior of neighboring hydrogens. An attempt of this nature is described in the accompanying paper.[43]

Materials and Methods

Protein preparation

Experiments used a double mutant of SN (P117G/H124L) with increased stability (from 6 kcal mol^{-1} for WT to 10 kcal mol^{-1} for the double mutant) so that the exchange of most hydrogens is not dominated by the transient global unfolding. The SN double mutant was purified as described before.[8]

HX rate determination

NMR HX measurements were done at 20 °C using a 500 MHz magnet with Varian cold probe. ^2H to ^1H exchange was measured by 2D HSQC in real time over the pH range 7.0–9.5 and by quenched stop flow at pH 9.94 as previously described.[8] Rates were determined by fitting crosspeak intensity as a function of time to a single exponential. ^1H-^1H exchange was measured using the Cleanex-PM pulse sequence[35] with mixing times of 4, 5, 6, 7, 8, 10, 15, and 20 ms over the pH range 4.9–11.26 at approximately half pH increments.

A modified data analysis was used to improve the accuracy of Cleanex results. Normalized peak volumes for ^1H-^1H data collected using the Cleanex-PM pulse sequence have been reported to fit Eq. (1).

$$V(t)/V_0 = \frac{f\,k_{ex}}{(k_{ex} + R_{1a} + R_{1b})}\left[e^{-R_{1b}t} - e^{-(k_{ex}+R_{1a})t}\right] \quad (1)$$

Values for f, the fraction of H_2O that recovers between pulses, and $R_{1b,}$ the solvent relaxation rate (residue and pH-independent) were determined experimentally at our conditions to be 0.54 and 0.6 s^{-1}, respectively. The HX rate, k_{ex}, and the hydrogen relaxation rate R_{1a} (residue-specific but pH-independent) were then determined by fitting measured data to Eq. (1).

Due to the nonlinear nature of Eq. (1), the k_{ex} value derived from fitting is highly dependent on the choice of initial coefficient values. Other groups have avoided this problem by simply approximating k_{ex} from the initial time-dependent slope. However, that approach introduces a systematic error and would not use all of the time-dependent HX data and the large amount of pH-dependent data available to us. We fit the entire HX dataset for each hydrogen by using successively improved approximations to Eq. (1). k_{ex} was first approximated for each residue at each pH by setting its starting value equal to the initial slope divided by f. In a second round, k_{ex} was fit for each residue at each pH using Eq. (1) and assuming $R_{1a} = 0$. k_{ex} and R_{1a} were then fit by using k_{ex} from the previous round as the starting k_{ex} value and 50 s^{-1} as the starting R_{1a} value. k_{ex} and R_{1a} were fit for each residue at all pH's simultaneously based on the knowledge that k_{ex} increases by 10-fold per pH unit and R_{1a} is independent of pH. This provides the final R_{1a} rate for each residue and the starting k_{ex} rates for a final round of fitting, done for each residue at each pH. All fitting was done using the Matlab v2008a function 1sqnonlin. In comparison with the usual initial slope method, this approach yields rates that are systematically faster, especially for fast exchanging hydrogens (Fig. 5).

At low pH when $k_{ex} < 1$ s^{-1}, we observed for most amides a low level pH-independent background signal not described in Eq. (1). This signal, when it could be measured for each amide at low pH, or the global average when it could not, was subtracted from all pH-dependent time points prior to rate determination. The improved data utilization of this

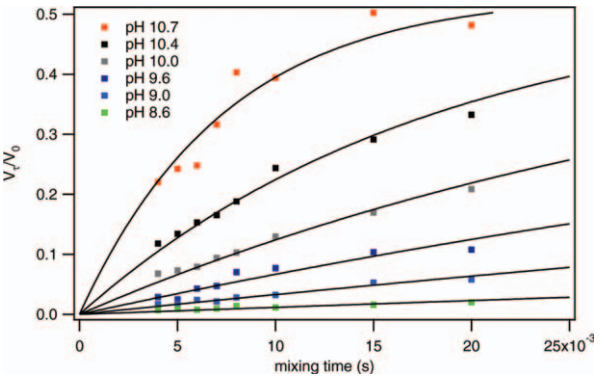

Figure 5. ^{1}H-^{1}H (Cleanex-PM) rate determination. Gly86 is presented as a typical example of the method described for fitting Cleanex-PM data to the complete Eq. (2). Rates obtained are faster than found by the initial slope method, especially at higher pH. The validity of the fitting method is demonstrated by the good agreement of many hydrogens with their expected pH dependence (Fig. 1).

analysis for fast rates is illustrated in Figure 5. The accuracy obtained can be seen in the match of all data to the theoretical pH dependence in Figure 1.

HX interpretation

HX behavior has generally been considered in terms of the Linderstrøm-Lang conformational closed to open kinetic picture in Scheme 1. Hydrogens in the closed state cannot exchange at all but require a deprotection opening reaction to become exchange competent. Once transient opening occurs, a kinetic competition ensues between exchange and reclosing. When structure is stable ($k_{cl} > k_{op}$) and reclosing is fast ($k_{cl} > k_{ch}$), the measured exchange rate, k_{ex}, depends on k_{ch} multiplied down by the fraction of time open, as in Eq. (2). This is the so-called EX2, bimolecular exchange, case since the chemical exchange rate, k_{ch}, is proportional to the concentration of solvent HX catalyst, namely hydroxide ion over the pH range studied here. This dependence generates the unit slope of the rate – pH behavior in Figure 1.

$$k_{ex} = k_{op}/(k_{op} + 1)k_{ch} \sim k_{op}k_{ch} \quad (2)$$

For EX2 exchange, HX rates are reported here in terms of the HX protection factor, P_f, obtained as the ratio of the rate expected for a given hydrogen when it is freely exposed to solvent divided by the measured rate, as in Eq. (3).

$$P_f = (k_{op} + 1)/k_{op} = k_{ch}/k_{ex} \quad (3)$$

With increasing pH, k_{ch} increases and may exceed k_{cl}. In this so-called EX1 case, k_{ex} reaches a limiting rate equal to k_{op}. The slowest exchanging SN hydrogens in Figure 1 exhibit an EX2 to EX1 transition, which will occur only for protected hydrogens when structural reclosing is slow relative to k_{ch}.

Structure-based calculations

Structure calculations were based on the SN crystal structure (1SNO) with Pro117 mutated to glycine by deleting extra atoms. Crystallographic waters were removed unless otherwise specified and hydrogens were added using CHARMM. Solvent accessible surface area (SASA) was calculated using Surfcv[48] with a 1.4 Å rolling ball radius and CHARMM22 atomic radii.

Electrostatic Poisson-Boltzmann continuum dielectric calculations were performed with Qnifft.[49,50] We used the same parameters previously described by LeMaster *et al.*,[14,41] namely CHARMM22 atomic radii and charge distribution, an internal dielectric of 3 and an external dielectric of 78.5. The probe size was set to 1.4 Å with a grid size of 193 and scaling was set to 3.0. Temperature was 298 K with a monovalent salt concentration of 150 m*M*.

HX rate predictions

Structure-based predictions for individual residue HX rates in P117G/H124L SN were supplied by M. Vendruscolo and by L. Tong and V. Hilser, based on their published methods.

Acknowledgments

The authors thank L. Tong, V. Hilser, and M. Vendruscolo for supplying the model predictions in Figure 4 and George Rose for helpful discussion.

References

1. Eigen M (1964) Proton transfer, acid-base catalysis, and enzymatic hydrolysis. Angew Chem Intl Ed Engl 3:1–19.
2. Bai Y, Milne JS, Mayne L, Englander SW (1993) Primary structure effects on peptide group hydrogen exchange. Proteins 17:75–86.
3. Connelly GP, Bai Y, Jeng MF, Englander SW (1993) Isotope effects in peptide group hydrogen exchange. Proteins 17:87–92.
4. Linderstrøm-Lang KU, Schellman JA. Protein structure and enzyme activity. In: Boyer PD, Lardy H, Myrback K, Eds. (1959) The enzymes. New York: Academic Press, pp 443–510.
5. Hvidt A, Nielsen SO (1966) Hydrogen exchange in proteins. Adv Protein Chem 21:287–386.
6. Englander SW, Kallenbach NR (1983) Hydrogen exchange and structural dynamics of proteins and nucleic-acids. Q Rev Biophys 16:521–655.
7. Wrabl JO (1999) Investigations of denatured state structure and m-value effects in staphylococcal nuclease. USA: The Johns Hopkins University, pp. 199.
8. Bédard S, Mayne LC, Peterson RW, Wand AJ, Englander SW (2008) The foldon substructure of staphylococcal nuclease. J Mol Biol 376:1142–1154.
9. Lumry R, Rosenberg A (1975) The mobile defect hypothesis of protein function. Col Int C N R S L'Eau Syst Biol 246:55–63.
10. Richards FM (1979) Packing defects, cavities, volume fluctuations, and access to the interior of proteins, including some general comments on surface area and protein structure. Carlsberg Res Commun 44:47–63.
11. Woodward C, Simon I, Tuchsen E (1982) Hydrogen-exchange and the dynamic structure of proteins. Mol Cell Biochem 48:135–160.

12. Matthew J, Richards F (1983) The pH dependence of hydrogen exchange in proteins. J Biol Chem 258: 3039–3044.
13. Fogolari F, Esposito G, Viglino P, Briggs JM, McCammon JA (1998) pK_a shift effects on backbone amide base-catalyzed hydrogen exchange rates in peptides. J Am Chem Soc 120:3735–3738.
14. LeMaster DM, Anderson JS, Hernandez G (2009) Peptide conformer acidity analysis of protein flexibility monitored by hydrogen exchange. Biochemistry 48: 9256–9265.
15. Anderson JS, LeMaster DM, Hernandez G (2006) Electrostatic potential energy within a protein monitored by metal charge-dependent hydrogen exchange. Biophys J 91:L93–L95.
16. Hilser VJ, Freire E (1996) Structure-based calculation of the equilibrium folding pathway of proteins: correlation with hydrogen-exchange protection factors. J Mol Biol 262:756–772.
17. Shirley WA, Brooks CL (1997) Curious structure in "canonical" alanine-based peptides. Proteins 28:59–71.
18. Sheinerman FB, Brooks CL (1998) Calculations on folding of segment b1 of streptococcal protein G. J Mol Biol 278:439–456.
19. Bahar I, Wallqvist A, Covell DG, Jernigan RL (1998) Correlation between native-state hydrogen exchange and cooperative residue fluctuations from a simple model. Biochemistry 37:1067–1075.
20. Garcia AE, Hummer G (1999) Conformational dynamics of cytochrome c: correlation to hydrogen exchange. Proteins 36:175–191.
21. Wooll JO, Wrabl JO, Hilser VJ (2000) Ensemble modulation as an origin of denaturant-independent hydrogen exchange in proteins. J Mol Biol 301:247–256.
22. Dempsey CE (2001) Hydrogen exchange in peptides and proteins using NMR spectroscopy. Prog NMR Spectrosc 39:135–170.
23. Dixon RDS, Chen YW, Feng D, Khare SD, Prutzman KC, Schaller MD, Campbell SL, Dokholyan NV (2004) New insights into fak signaling and localization based on detection of a fat domain folding intermediate. Structure 12:2161–2171.
24. Vertrees J, Barritt P, Whitten S, Hilser VJ (2005) Corex/best server: a web browser-based program that calculates regional stability variations within protein structures. Bioinformatics 21:3318–3319.
25. Vertrees J, Wrabl JO, Hilser VJ (2009) Energetic profiling of protein folds. Methods in enzymology 455(A):299–327.
26. Gsponer J, Hopearuoho H, Whittaker SBM, Spence GR, Moore GR, Paci E, Radford SE, Vendruscolo M (2006) Determination of an ensemble of structures representing the intermediate state of the bacterial immunity protein Im7. Proc Natl Acad Sci USA 103:99–104.
27. Tartaglia GG, Cavalli A, Vendruscolo M (2007) Prediction of local structural stabilities of proteins from their amino acid sequences. Structure 15:139–143.
28. Vendrusculo M, Paci E, Dobson CM, Karplus M (2003) Rare fluctuations of native proteins sampled by equilibrium hydrogen exchange. J Am Chem Soc 125: 15686–15687.
29. Best RB, Vendruscolo M (2006) Structural interpretation of hydrogen exchange protection factors in proteins: characterization of the native state fluctuations of CI2. Structure 14:97–106.
30. Vendruscolo M, Dobson CM (2006) Dynamic visions of enzymatic reactions. Science 313:1586–1587.
31. Dovidchenko NV, Lobanov MY, Garbuzynskiy SO, Galzitskaya OV (2009) Prediction of amino acid residues protected from hydrogen-deuterium exchange in a protein chain. Biochemistry-Moscow 74:888–897.
32. Hilser VJ (2010) An ensemble view of allostery. Science 327:653–654.
33. Wrabl JO, Gu JN, Liu T, Schrank TP, Whitten ST, Hilser VJ (2011) The role of protein conformational fluctuations in allostery, function, and evolution. Biophys Chem 159:129–141.
34. Craig PO, Lätzer J, Weinkam P, Hoffman RMB, Ferreiro DU, Komives EA, Wolynes PG (2011) Prediction of native-state hydrogen exchange from perfectly funneled energy landscapes. J Am Chem Soc 133 17463–17472.
35. Hwang TL, van Zijl PC, Mori S (1998) Accurate quantitation of water-amide proton exchange rates using the phase-modulated clean chemical exchange (cleanex-pm) approach with a fast-HSQC (fHSQC) detection scheme. J Biomol NMR 11:221–226.
36. Molday RS, Englander SW, Kallen RG (1972) Primary structure effects on peptide group hydrogen exchange. Biochemistry 11:150–158.
37. Truhlar SME, Croy CH, Torpey JW, Koeppe JR, Komives EA (2006) Solvent accessibility of protein surfaces by amide H/H2 exchange MALDI-TOF mass spectrometry. J Am Soc Mass Spectrom 17:1490–1497.
38. Bai Y, Sosnick TR, Mayne L, Englander SW (1995) Protein folding intermediates: native-state hydrogen exchange. Science 269:192–197.
39. Bai Y, Englander JJ, Mayne L, Milne JS, Englander SW (1995) Thermodynamic parameters from hydrogen exchange measurements. Energ Biol Macromol 259:344–356.
40. Hernandez G, Anderson JS, LeMaster DM (2009) Polarization and polarizability assessed by protein amide acidity. Biochemistry 48:6482–6494.
41. Anderson JS, Hernandez G, Lemaster DM (2008) A billion-fold range in acidity for the solvent-exposed amides of *Pyrococcus furiosus* rubredoxin. Biochemistry 47:6178–6188.
42. Hilser VJ, Freire E (1997) Predicting the equilibrium protein folding pathway: structure-based analysis of staphylococcal nuclease. Proteins 27:171–183.
43. Skinner JJ, Lim WK, Bédard S, Black BE, Englander SW (2012) Protein dynamics viewed by hydrogen exchange. Protein Sci 21:996–1005.
44. Marx D, Chandra A, Tuckerman ME (2010) Aqueous basic solutions: hydroxide solvation, structural diffusion, and comparison to the hydrated proton. Chem Rev 110:2174–2216.
45. Avbelj F, Baldwin RL (2009) Origin of the change in solvation enthalpy of the peptide group when neighboring peptide groups are added. Proc Natl Acad Sci USA 106:3137–3141.
46. Avbelj F, Baldwin RL (2004) Origin of the neighboring residue effect on peptide backbone conformation. Proc Natl Acad Sci USA 101:10967–10972.
47. Hilser VJ. Modeling the native state ensemble. In: Murphy KP, Ed. (2001) Proteins. Totowa, NJ: Humana Press, pp. 93–116.
48. Nicholls A, Sharp KA, Honig B (1991) Protein folding and association: insights from the interfacial and thermodynamic properties of hydrocarbons. Proteins 11: 281–296.
49. Gilson MK, Sharp KA, Honig BH (1988) Calculating the electrostatic potential of molecules in solution—method and error assessment. J Comput Chem 9: 327–335.
50. Sharp KA, Friedman RA, Misra V, Hecht J, Honig B (1995) Salt effects on polyelectrolyte-ligand binding: comparison of Poisson-Boltzmann, and limiting law/counterion binding models. Biopolymers 36:245–262.